Synthesis and characterisation of a new graphitic C–S compound obtained by high pressure decomposition of CS2

Stefan Klotz, B. Baptiste, T. Hattori, S.M. Feng, Ch Jin, K. Béneut, J.M. Guigner, I. Estève

Published in: Carbon 185 491-500 (2021)

Synthesis and characterisation of a new graphitic C-S compound obtained by high pressure decomposition of CS_2

S. Klotz[a,*], B. Baptiste[a], T. Hattori[b], S.M. Feng[c], Ch. Jin[c], K. Béneut[a], J.M. Guigner[a], I. Estève[a]

[a] Institut de Minéralogie, de Physique des Matériaux et de Cosmochimie (IMPMC), CNRS UMR7590, Sorbonne Université, 4 Place Jussieu, 75252 Paris, France

[b] J-PARC Center, Japan Atomic Energy Agency, 2-4 Shirakata, Tokai, Ibaraki 319-1195, Japan

[c] Institute of Physics, Chinese Academy of Sciences (IOPCAS), School of Physics, University of Chinese Academy of Sciences(UCAS), Beijing 100190, China

Abstract

Carbon disulphide (CS_2) is, together with its closest analogue CO_2, one of the simplest molecular systems made of double covalent bonds. Under high pressure, the molecular structure is expected to break up to form extended crystalline or polymeric solids. Here we show that by compression at 300 K to ~10 GPa (100 kbar) using large-volume high pressure techniques, a sudden reaction leads to a mixture of pure sulphur and a well-defined compound with stoichiometry close to C_2S which can be recovered to ambient pressure. We present neutron and x-ray diffraction as well as Raman data which show that this material

* Corresponding author; e-mail : Stefan.Klotz@upmc.fr

consists of sulphur bonded to sp^2 graphite layers of nanometric dimensions. The compound is a semiconductor with a gap of 45 meV, as revealed by temperature dependent resistivity measurements, and annealing at temperatures above 200 °C allows to reduce its sulphur content up to $C_{10}S$. Its structural and electronic properties are fundamentally different to "Bridgman black" reported from previous high pressure experiments on CS_2.

Keywords: graphite, high pressure, carbon disulphide, neutron scattering, Raman scattering.

1. Introduction

The general trend in molecular systems under compression is that they solidify (in most cases crystallise) in the GPa range and at sufficient high pressure ultimately form extended crystalline or amorphous compounds as the molecules break up [1]. These high pressure solids have vastly different electronic properties compared to the starting material and in some cases can be quenched to ambient pressure where they may have useful properties. A well-known example is carbon-monoxide (CO) which transform under pressure of 5 GPa to a polymeric compound which can be recovered to atmospheric pressure and which is a high-density energy material [2]. Another case is CS_2, a colourless liquid with a strong odour which is isostructural to CO_2. Following a reaction route indicated by Bridgman [3], CS_2 transforms at 3-5 GPa and ~250 °C into a black solid (« Bridgman black ») which can be recovered to ambient pressure and temperature. Analysis suggests that it consists of a disordered 3D network with the same stoichiometry as CS_2 and highly crosslinked chains with both single and double C-S bonds [4-11]. The material is a semiconductor [6] with a poor electrical conductivity of 10^{-13} $Ohm^{-1}cm^{-1}$. Compression at 300 K (without heating) in a diamond anvil cell leads to a

transition at 8-10 GPa which is governed by kinetics [9], and it appears that the structure of the polymer depends on the specific experimental conditions it has formed [10].

Here we report the transformation of CS_2 in the 10 GPa range, at ambient temperature, using a large-volume ("Paris-Edinburgh") pressure device. This technique allows to load and compress ~100 mm^3 liquid samples, i.e. macroscopic quantities, between two opposed anvils and a metallic gaskets. It can be used for both in-situ characterisation by neutron and x-ray diffraction as well as ex-situ sample synthesis, see ref. [12] for a detailed description of the method. Our investigations involved two types of experiments: In a first measurement, the transformation of CS_2 was observed and studied by in-situ neutron diffraction to 9 GPa. These revealed a sudden transition at ~ 8 GPa from a crystalline molecular solid to a disordered compound which can be recovered to ambient pressure. In a second type of experiments, the recoverability of the sample was exploited to produce in several loadings a considerable amount of material (~0.5 cm^3) at atmospheric pressure. The availability of such macroscopic sample quantities at ambient pressure, outside the pressure cell, then enabled us an in-depth characterisation of the reaction product by applying a variety of techniques, in particular x-ray and additional neutron diffraction, Raman scattering, infrared absorption, density and resistivity measurements.

2. Experimental

2.1 Neutron diffraction at ambient and high pressure

In-situ high pressure diffraction measurements were carried out at the PLANET beamline of the Japanese neutron Facility MLF at J-PARC, Tokai, Ibaraki [13] using a VX4 Paris-Edinburgh press [12]. Approximately 30 mm^3 of CS_2 purchased from Wako Pure Chemical Industries Co. Ltd (Japan) was loaded into double-toroidal sintered diamond anvils and null-scattering TiZr

gaskets. The sample was then compressed at 300 K in steps of 1-2 GPa, up to ~8 GPa where it transformed suddenly. Pressures were determined to a precision of ± 1 GPa by the load on the anvils and a pre-determined calibration curve. Data in the crystalline phase (below 8 GPa) were analysed by Rietveld refinement using FullProf [14]. Once the transformation occurred, the sample was decompressed in steps to 0 GPa, again with data taken during the download. Neutron diffraction patterns at ambient pressure from recovered and purified samples (see sections 2.2 and 2.3) were collected in a vanadium can. Pair correlation functions g(r) of the patterns S(Q) were obtained with the software package *0529_FourierTranslation.exe* developed by Kyushu University/Dr. Kohara (SPring8) (Japan) using number densities of ρ_0 =0.01419/Å^3 and ρ_0 =0.0104/Å^3 for the un-annealed and annealed samples, respectively.

2.2 *Ex-situ* (off-line) sample production

Since the *in-situ* neutron data demonstrated that the sample obtained at high pressure can be recovered to ambient pressure, a series of samples were produced in off-line runs using single-toroidal tungsten carbide anvils [12] and copper beryllium gaskets, with a VX3 Paris-Edinburgh load-frame. This different anvil/gasket configuration allowed a much larger sample volume of initially 106 mm^3, as well an easy extraction of the sample pellet from the metallic gasket. Again, the transition occurred suddenly and was observable by and audible “click” and a drop in load at 72 ± 3 tonnes on the anvils, which corresponds to 7-8 GPa according to a calibration curve for such anvils. The transition is perfectly reproducible and was observed in at least 20 runs, half of them in runs concerned by this report. Samples were decompressed to ambient pressure at a speed of ~ 1 GPa/min. Liquid CS_2 was purchased from ARCOS ORGANICS (99.9%) and Tokyo Chemical Industry (98%) and loaded into the cell using a previously described

method [15]. The source of the samples had no observable influence on the outcome of the experiments.

2.3 Sample purification, determination of density and stoichiometry.

Visible observation of the sample after extraction from the pressure cell revealed an inhomogeneous compound of crystalline sulphur in a matrix of black material (see Results section). To remove the sulphur, the pellet was filed, then thoroughly grinded in liquid CS_2 and stirred in a high-power ultrasonic bath to dissolve the sulphur. The turbid fluid was centrifuged at 7500 rpm to sediment the black micrometer-size particles, and the whole procedure was repeated a second time with fresh CS_2. After drying in vacuum, the powder appeared homogeneous and no trace of crystalline sulphur could be detected neither visually nor by Raman scattering.

The average density of the inhomogeneous pellet was then measured by Archimedes' method using distilled water and an electronic balance model L432 from BEL Engineering (resolution: 1 mg) and its associated DENS-01 density kit. Given the initial mass and volume of the pellet, the mass of the powder after removal of sulphur as well as the known density of crystalline sulphur, the density and stoichiometry x and of the remaining homogenous material C_xS could be easily determined to an accuracy of 2% and 5%, respectively.

2.4 Raman and infrared measurements

Raman experiments were carried out using a confocal in-house optical set-up using a Jobin-Yvon/Horiba HR-460 spectrometer equipped with a monochromator with 1500 grooves/mm and a Peltier-cooled Andor CCD. Raman scattering was excited by a continuous argon ion laser

emitting at 514.5 nm and focused onto a spot of about 2 µm. Spectra were collected in backscattering geometry with maximal 7 mW laser power on the powder sample. Infrared measurements were performed on a Bruker IFS66V/S Fourier transform infrared spectrometer working in vacuum and aligned in transmission geometry. Spectra were acquired in the frequency region 600-8000 cm^{-1} with resolution of 4 cm^{-1} and accumulation of 10 scans using the mid infrared instrumental configuration with Globar, KBr and MCT as respectively source, beam splitter and detector. A homogeneous pellet of 13 mm diameter was prepared by mixing 1 mg powder sample with 200 mg grinded and dried KBr powder as transparent matrix material.

2.5 X-ray diffraction and gravimetric measurements

X-ray diffraction data of the purified samples were obtained on an Xcalibur-S 4-circle diffractometer from Rigaku (Agilent) with a Sapphire CCD detector and a Mo anode (17.4 keV), and the samples filled into a 1 mm kapton capillary. Diffraction patterns from the sample and the empty capillary were collected up to Q=15 $Å^{-1}$ in transmission geometry and the azimuthal integration of the 2D patterns was done with the CrysalisPro software (CrysAlisPro 1.171.38.46, Rigaku Oxford Diffraction, 2015). After subtraction of the capillary contribution, the pair distribution function was obtained from the Fourier transform of the scattering function S(Q) using the PDFgetx3 program [16]. Thermogravimetric measurements used a Q600 SDT from TA Instruments with Pt crucibles under nitrogen flow. The sample with initially a mass of approximately 10 mg was heated at a rate of 3 K/min from 20 °C to 700 °C.

2.6 Transmission and Scanning Electron Microscopy (TEM/SEM)

Transmission Electron Microscopy (TEM) measurements were carried out using a JEOL 2100F field emission gun instrument operating at 200 kV in combination with an UltraScan 4000

Gatan CCD camera and an energy dispersive x-ray detector with 140 eV resolution for elemental mapping. For Scanning Electron Microscopy (SEM) measurements we used a Zeiss Ultra 55 field emission gun SEM operated at 15 kV. Backscattered electron or secondary electrons modes were applied to investigate the morphology. Energy dispersive X-ray spectrometry (EDXS) point analysis was carried out at a working distance of 7.5 mm using an EDXS QUANTAX system equipped with a silicon drift detector XFlash 4010 (Bruker). Data were processed with the software Esprit (Bruker).

2.7 Electrical resistivity measurements

Four-probe DC resistivity measurements were carried out with a laboratory-made sample holder consisting of two electrically insulated Al-plates which compact the powder sample on a strip of 7 mm length and 0.3x1.0 mm^2 cross section. The sample holder was then attached and electrically contacted to a standard sample "puck" with its associated sample stick from Quantum Design. The measurements were carried out with a PPMS (Quantum Design) between 2 and 300 K using a current limit of 100 μA and a cooling/heating rate of 1 K/min. Varying the current showed ohmic behaviour of the resistivity.

3. Results

We first report the *in-situ* observation of the high pressure transformation of CS_2 by neutron diffraction (Fig. 1). The crystalline phase below 8 GPa can be well fitted by the known *Cmca* structure [17] with no detectable contaminant in the diffraction patterns. Rietveld refinements show an anisotropic compression of the structure with no change of the C=S bond length to within ± 0.01 Å (the precision of the technique) nor a change in the orientation of the molecule in the unit cell. At a load of 71 tonnes corresponding to 7.9 GPa, the load suddenly dropped by 1 tonne and the diffraction pattern revealed a transformation to a

strongly disordered (amorphous) solid. Diffraction patterns were collected for the following 12 hours where no further change could be observed, indicating that the transition was complete.

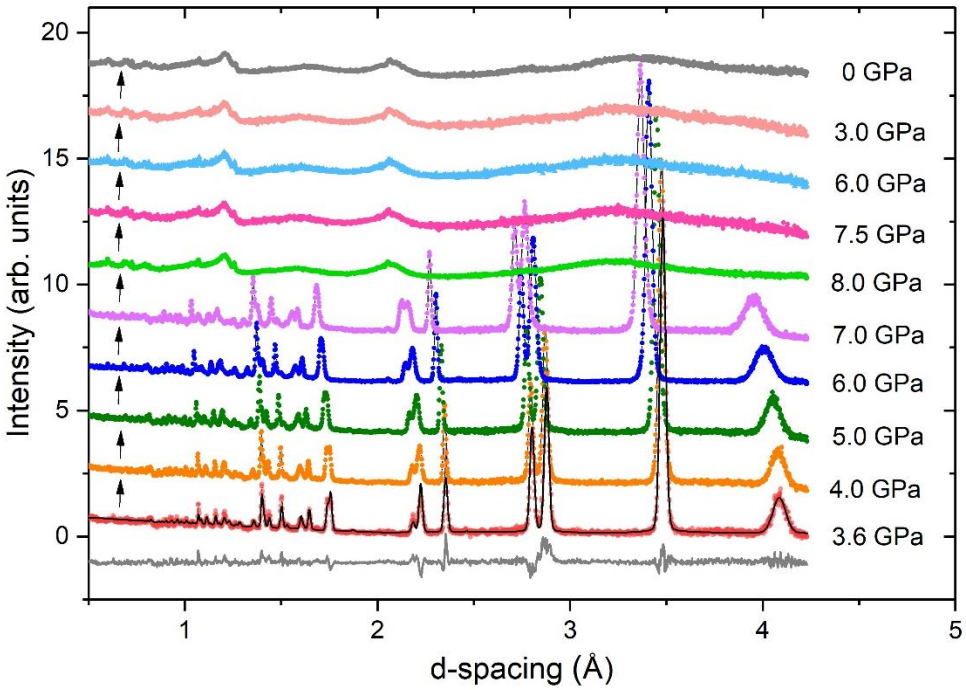

Fig. 1 Neutron diffraction patterns of CS_2 as a function of pressure. Patterns were shifted vertically for clarity. Arrows indicate sequence of data collection. The line through the data at 3.6 GPa is a Rietveld fit and the grey line below the difference curve. Errors in pressure values are estimated to ± 0.5 GPa in the upstroke and ± 1.5 GPa in the downstroke.

The sample was then decompressed in 4 steps (60, 40, 20, 5 tonne corresponding to an estimated 7.5, 6, 2 and 0 GPa, respectively) and no changes could be observed apart from a trivial shift of all features to larger *d*-spacings as the load (pressure) is decreased. The sample obtained at high pressure is hence recoverable to ambient pressure, with no apparent modifications except a decrease in density.

After these observations, the experiment was repeated with a different gasket-anvil setup allowing three times more volume per loading and an easy extraction of the recovered sample. The aim was to produce larger sample quantities, at ambient pressure, which allow a detailed characterisation by various other methods which cannot be carried out in the pressure cell. Runs using this setup gave reproducibly spherical black spheres of ca. 6 mm diameter inside the metallic gasket with no trace of remaining liquid (Fig. 2). Observation under a laboratory microscope shows an inhomogeneous sample with yellowish streaks within a matrix of black material. Micro-Raman measurements identified the yellow component as crystalline octa-sulphur, as expected, by comparison with the known Raman spectrum. Since we were interested only in the black homogeneous materiel, the sulphur was removed by dissolving the grinded powder in liquid CS_2, as explained above. It was checked by Raman scattering that this procedure does not modify the remaining component. The density of the initial (inhomogeneous) pellet was determined by Archimedes' method (see above) and gave a value of 1.95 ± 0.03 g/cm^3. From this and the mass of the powder after removing the crystalline sulphur, a composition of approximately C_2S and a density of 1.76 ± 0.03 g/cm^3 was determined for the remaining compound. This value might be compared to the density of pure graphite (2.26 g/cm^3) and pure crystalline sulphur (2.07 g/cm^3). For simplicity, we will call this compound "C_2S" in the following.

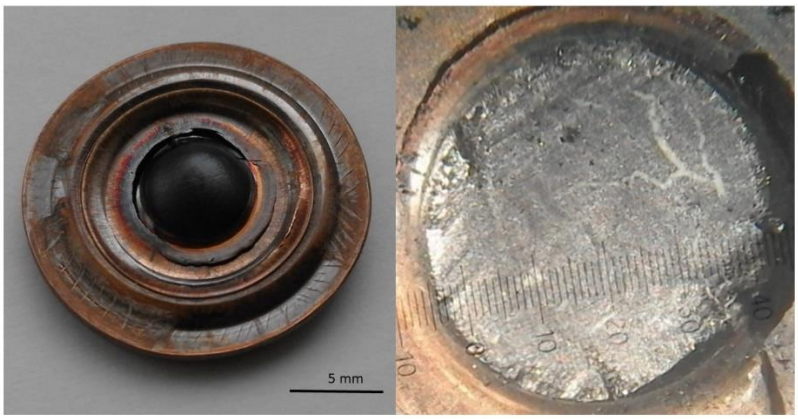

Fig. 2. Left: Sample (black sphere in the centre) surrounded by the brownish metallic gasket, after extraction from the pressure cell. Right: Close-up view on the sample, after filing the pellet to obtain a flat surface. Note the yellow streaks from crystalline octo-sulphur.

The Raman spectrum (Fig. 3) of this purified black powder revealed immediately a nano-sized graphitic compound, i.e. a material made of sheets of carbon on a honeycomb lattice. Such material, which includes pyrolytic graphite and graphene, has been extremely well characterized by Raman scattering [18-20]. Its characteristic fingerprints are: The G-peak at 1586 cm^{-1}, the D-band at 1350 cm^{-1}, the 2D peak at 2690 cm^{-1} as well as an additional feature at 2940 cm^{-1} which appears in material with large disorder. The ratio of the D and G peak varies with the particle size and can be used to determine the average linear dimension of the carbon sheets [19] which gave ~25 Å in our case. In addition, the position of the G-band at 1585 cm^{-1} indicates a pile-up of only few carbon-layers in each crystal [20].

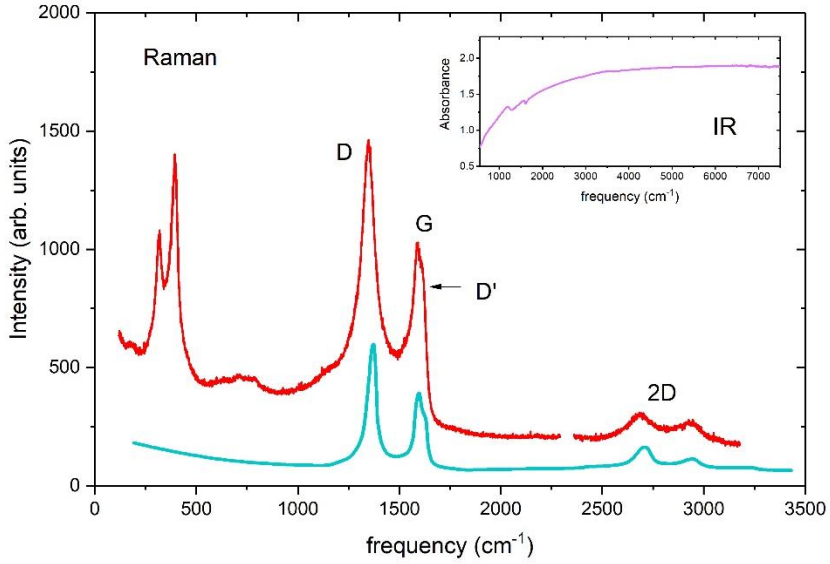

Figure 3: Raman spectra (main figure, upper red curve) and infrared absorbance (inset) of C_2S. The lower (blue) Raman spectrum are published data of disordered graphite [18] (called "glassy carbon" in [18]).

A significant difference compared to pure graphite or its various disordered forms is the existence of two intense peaks at 318 and 394 cm^{-1} which are absent in any of the latter materials. The peaks cannot be assigned to modes of remaining CS_2, nor to vibrations of residual crystalline sulphur, nor to those of S_8 or even S_2 monomers which have no modes between 250 and 410 cm^{-1} [21]. Since SEM and TEM measurements (see further below) show the presence of only two elements, carbon and sulphur, these modes have to be ascribed to vibration of C-S bonds formed between the carbon sheet and sulphur atoms. In contrast to the Raman data, the measured infrared absorbance in the 500-7000 cm^{-1} range (inset fig. 3) is almost featureless showing only two weak, broad and distorted features of at 1200 cm^{-1} and 1575 cm^{-1}. The latter is reminiscent to one of the two IR active modes in graphite (868 cm^{-1} and 1588 cm^{-1}) [22]. Note that single-layered graphene has no IR mode at all.

To invest the thermal stability of the compound, thermogravimetric measurements were carried out between 20 and 700 °C, see fig. 4. It is found that C_2S starts to decompose at ~200 °C reaching the maximum speed of transformation at 260 °C. The transformation is complete at ~350 °C after which the sample has lost approximately 50% of its mass.

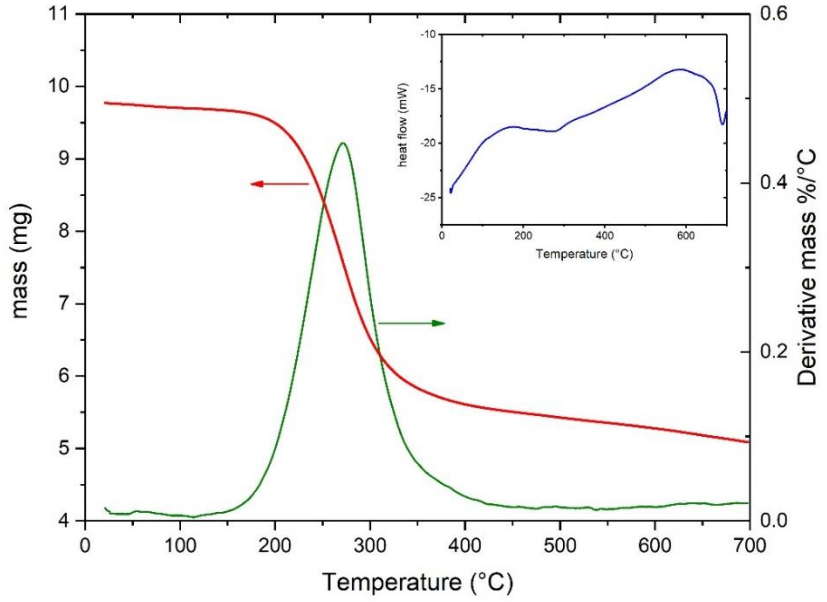

Fig. 4: Thermogravimetric data showing the loss of mass (red line, left scale) and its derivative (green line, right scale). The inset shows the associated heat transfer.

Since the initial stoichiometry (C_2S) as well as the change in mass is known, the annealed compound must still contain approximately 9 at% of sulphur, i.e. must have a composition of approximately $C_{10}S$. From the measured net heat flow during the transition we estimate the total amount of energy absorbed by the process to 3.7 J, i.e. 30 kJ per mole of released sulphur. This number is typically in the range of a strong van der Waals or ionic binding, i.e. the released sulphur is certainly not covalently bonded to carbon.

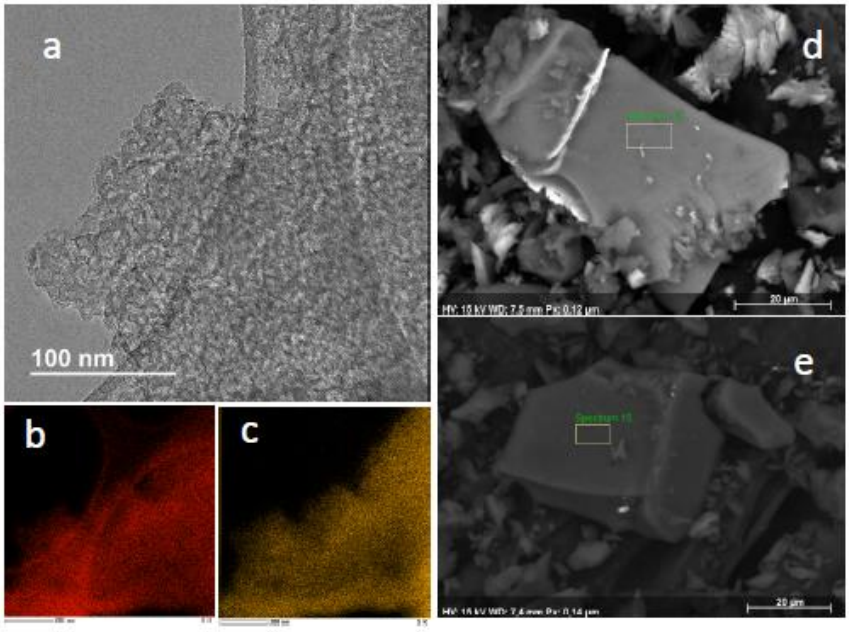

Figure 5: Representative TEM (a) and SEM (d,e) images of un-annealed (a,d) and annealed (e) samples. Image (b) and (c) show carbon and sulphur distribution in a similar flake as shown in (a). The convex structure visible in (a) and (b) is the sample holder, a Lacey carbon grid. The measured sulphur content is 33 at% in (d) and 14 at% in (e). TEM measurements were carried out at 80 K to reduce sample damage from electron bombardment.

Next, Scanning and Transmission Electron Microscopy (SEM and TEM, respectively) were carried out which support the average chemical compositions of the samples cited above but reveal a large spread in stoichiometry: Fig. 5 shows representative SEM and TEM images which find that the sulphur composition in the un-annealed sample ("C_2S") varies between typically 10 and 40 at% between different grains. In the annealed samples ("$C_{10}S$") it is between approximately 5 and 20 at%, and this composition remained approximately constant even for samples heated to 700 °C. Clearly, about 10% of the initial 30 at% sulphur must be tightly bonded to carbon. It was also found that the un-annealed samples were prone to changes in

247 their visual aspect during electron bombardment. This must hence be related to migration of
248 loosely bonded sulphur, the same fraction which can be removed by heating.

249 The structure of the powder samples was then determined by neutron and x-ray diffraction
250 applying a pdf analysis, as appropriate for disordered systems. We note that given a
251 composition of initially C_2S, the scattering of neutrons is almost completely dominated by
252 carbon (the coherent neutron cross sections of C and S are 5.6 barn and 1.0 barn, respectively,
253 i.e. S contributes less than 9% to the total intensity of the C_2S sample), whereas for x-rays,
254 sulphur (Z=16) governs the intensity compared to carbon (Z=6) (the scattering power for x-
255 rays is proportional to Z^2). The combined neutron and x-ray data have therefore the potential
256 to pinpoint structural features in quite detail.

257 Figure 6 shows a neutron diffraction pattern of C_2S and compares it to published neutron data
258 of what was called “turbostratic graphite” [23] (the terminology of disordered graphitic
259 systems varies widely between authors). The agreement is remarkable and leaves no doubt
260 on the 2D structure with its sp^2 carbon bonding. A pdf analysis (lower panel) confirms this
261 conclusion: The peaks at 1.41, 2.45, and 2.83 Å, 3.74 Å and 4.24 Å can all be identified with
262 the first four neighbour C-C distances of the 2D honeycomb lattice of graphite or graphene
263 with 2.41 Å edge length. However, one notices the complete absence of a peak at 3.35 Å which
264 would be expected for the inter-layer nearest neighbour C-C distance in graphite. In a
265 diffraction pattern it corresponds to the most intense reflection, the 002.

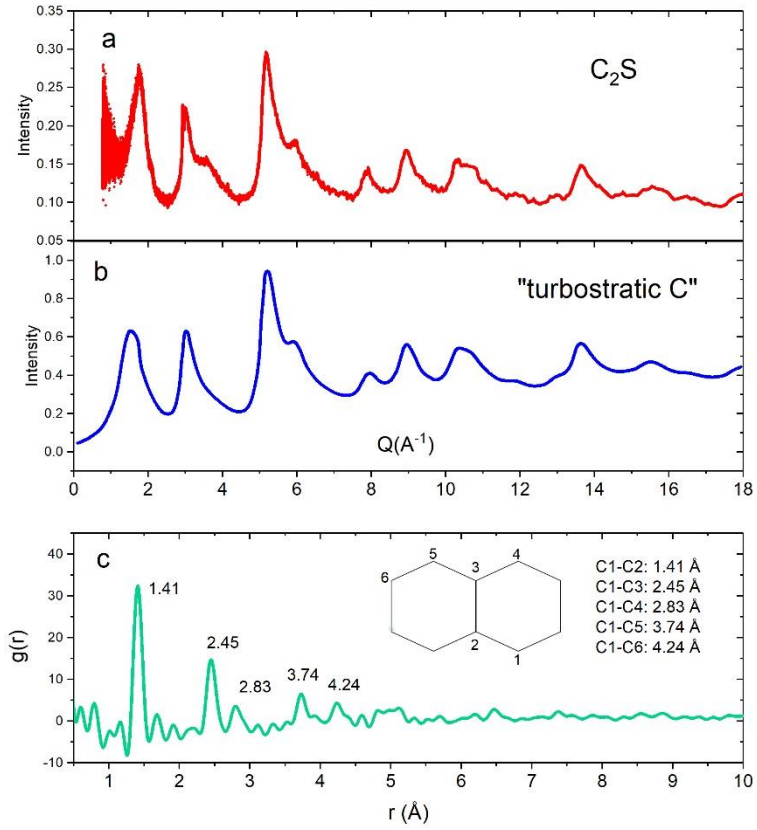

Fig. 6: Neutron diffraction pattern (a) compared to published neutron pattern of “turbostratic graphite” (b) [23]. The g(r) obtained from pdf analysis of (a) is shown in (c), together with the geometry in graphite/graphene and its five nearest in-plane carbon-carbon distances.

Figure 7 shows corresponding x-ray patterns along with a similar pdf analysis. Both patterns are from the same sample as used in the neutron study, but one pattern was collected after annealing at 250 °C for 10 h in a vacuum furnace. The difference between the annealed and the non-annealed sample identifies therefore unambiguously distances relate to sulphur only. The g(r) of the un-annealed sample shows a strong peak at 2.0 Å followed by a massif of several peaks between 3 and 5 Å. Other minor peaks, in particular at larger distances, may be artefacts of the data analysis given the limited Q-range. A comparison with the annealed sample reveals the disappearance of the most intense peak at 2.0 Å as well as a further peak at 3.3 Å. The

remaining peaks are at 1.47 Å, 1.87 Å, 2.43 Å, 2.83 Å, 3.80 Å and 4.24 Å are all – with the exceptions of the 1.87 Å peak – to within ~0.05 Å the same as found in the neutron data analysis. This confirms hence once again a hexagonal graphitic lattice.

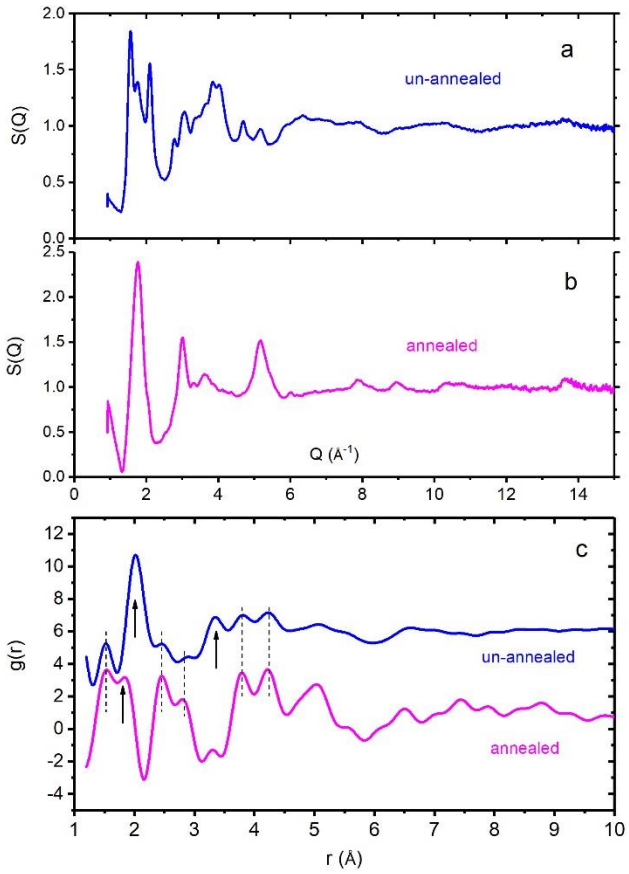

Fig. 7: X-ray diffraction pattern of (a) un-annealed and (b) annealed (250°C) samples. The corresponding g(r) obtained from a pdf analysis are shown in (c). The dashed vertical lines indicate distances already identified by neutron diffraction (see Fig. 6) and arrows indicate peaks related to sulphur. The curve for the un-annealed sample was shifted vertically for clarity.

Beyond any doubt, the two peaks at 2.0 Å and 3.30 Å in g(r) (arrows in Fig. 7c) must be related to sulphur, the fraction which is removed by heating to above 200 °C. The two distances are

in fact exactly what one would expect for an S_3 trimer with its well-known 107 degree S-S-S bond angle, a local geometry found in various sulphur allotropes [24]. The peak at 1.87 Å must also be related to sulphur, but to the ~ 10at% fraction which is still present after annealing, and its value corresponds exactly to what is expected for typical covalent C-S bonds. It is this fraction of sulphur which must be responsible for the low-energy Raman modes at 300-400 cm^{-1} since these exist even in the annealed samples. Indeed, frequencies in this range are typical for C-S bending modes [25,26].

A closer look at the three sharpest features in the diffraction pattern of fig. 7a reveals that their positions agree well with those of "polymeric sulphur" [27], in particular Tuinstra's "fibrous sulphur" labelled $S_{\omega 1}$ [28,29]. These are highly disordered, non-equilibrium states, usually obtained by quenching sulphur from the liquid and which do not dissolve in carbon disulphide. But in contrast to such reported bulk polymeric sulphur we do not see the associated infrared signature [27] in our samples, nor its decomposition [27] at 120 °C. From this we conclude that the majority of sulphur present in our samples cannot be a separate phase coexisting in a mainly carbon-rich matrix.

We have also investigated the electronic properties of un-annealed (C_2S) samples. Fig. 8 shows measurements of the dc-resistivity ρ and its temperature dependence between 5 and 300 K. We find a conductivity ($1/\rho$) of 0.1 $Ohm^{-1}cm^{-1}$ at 300 K which is 13 orders magnitude higher than reported from Bridgman's black [6]. The compound is a semiconductor. From the slope of the $\ln(\rho)$ vs 1/T Arrhenius plot at high temperatures (above 200 K) we derive a gap of 46 meV (inset of Fig. 8). At lower temperatures the same presentation deviates significantly from being linear. However, the T-dependence can be well fitted over the entire temperature range by a variable hopping range model [30] given by the expression:

$$\rho = \rho_0 \exp(T_0/T)^p$$

where p is a fitting parameter related to the dimension d of the hopping mechanisms by p=1/(1+d). We find p=0.43, i.e. d=1.3. This appears to be consistent with a structure where short range hopping occurs along a 1-dimensional C-C bond and where hopping over larger distances probe the 2-dimensional nature of the carbon sheets.

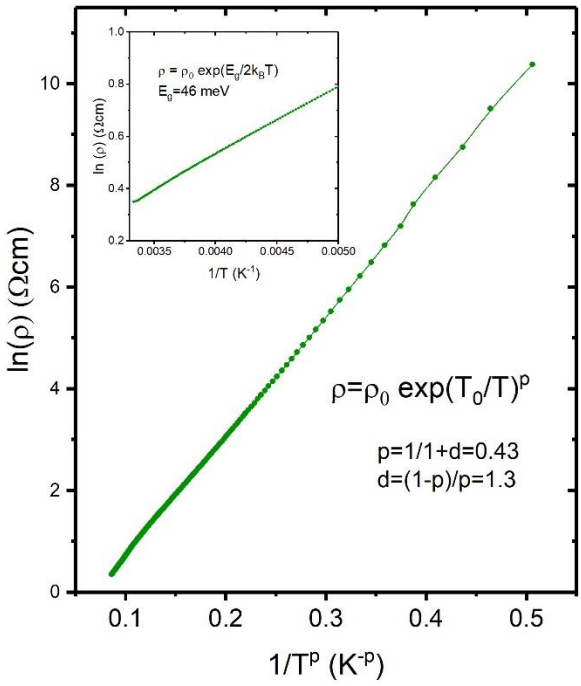

Figure 8: Temperature dependence of resistivity of C_2S. The main picture shows a fit to a variable range hopping model [30], the inset an Arrhenius-plot of the high temperature range to extract the conventional band gap E_g.

4. Discussion and conclusion

The emerging picture from these studies can hence be resumed as following: When liquid CS_2 is compressed at 300 K it crystallizes at 1.3 GPa. Further compression to 7-8 GPa leads to a

chemical reaction giving a mixture of pure crystalline sulphur and a compound with nanometric sp^2-bonded carbon layers, approximate composition of C_2S and a density of 1.76± 0.03 g/cm^3, see Fig. 9 for an illustration. Most of the sulphur remaining therein is weakly (van der Waals) bonded to the carbon sheets, is locally in form of S_3 trimers with some resemblance to a polymeric state and can be removed by heating to above 200 °C. The remaining 10 at% sulphur is strongly (covalently) bonded to the carbon backbone and gives rise to Raman modes in the 300-400 cm^{-1} range. It persists to temperatures of at least 700 °C. For chemical reasons, this type of sulphur is most likely bonded to carbon located at the edges of the carbon flakes. Indeed, a flake with 25 Å diameter (see above) contains approximately 200 carbon atoms from which ~ 30 are on edge positions, i.e. 14%. For a flake with 40 Å diameter, approximately 10% are on edge positions. In conclusion, given the wide distribution in the size of the flakes, these numbers are consistent with the measured average stoichiometry of $C_{10}S$.

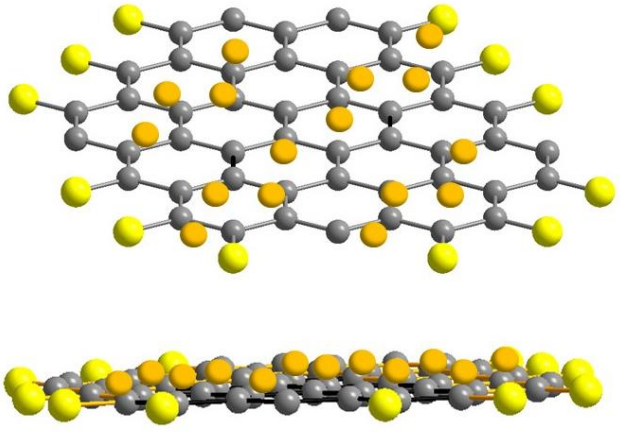

Fig. 9: Structural model of C_xS: Sulphur is attached to carbon sheets, either by van der Waals bonds (orange atoms) or by covalent bonds (yellow atoms), with average stoichiometry C_2S. Annealing at T>200 °C removes the van der Waals bonded species, leaving only covalently bonded sulphur resulting in an average composition of $C_{10}S$.

345 The question then arises what mechanism leads to the formation of C_xS instead of "Bridgman
346 black" as found in previous 300 K compression studies [8-11]. For this we note that carbon
347 disulphide has a positive formation enthalpy of +88.7 kJ/mole [31], i.e. the molecule is
348 inherently metastable. This contrast with its closest analogue, CO_2, which has a large negative
349 formation enthalpy of –393 kJ/mol [31]. As a result of this, its polymerisation or partial
350 decomposition is exothermic, and a reaction will self-propagate if the heat cannot be
351 evacuated rapidly. This is likely the case in large-volume pressure apparatuses where the
352 sample surface/volume ratio is small, in contrast to the geometry in diamond anvil cells [8-11]
353 where the anvils, in addition, are excellent heat sinks. The sample in our high pressure method
354 is therefore likely to self-heat to beyond the stability of Bridgman black, potentially into the
355 P/T region which currently is believed to be "carbon+sulphur" [10] or "CS_2+sulphur" [9]. If this
356 is correct, our work would mean that in the reaction product so far believed to be simply
357 "carbon" is in fact a new carbon-sulphur compound with stoichiometry C_2S.

358 Finally, this new compound may be compared to other known graphitic compounds. Given
359 the absence of sharp Bragg peaks reminiscent to graphite, in particular the absence of a sharp
360 002 reflection (see above), the compound is not a canonical "graphite intercalated compound"
361 (GIC) in the strict sense. However, C_xS bears some resemblance with graphene oxide, though
362 its structure is fundamentally simpler since it contains only carbon and sulphur with no oxygen
363 functional groups such as hydroxyl. Its closest relative could be a compound termed "RGO/S"
364 [32], judged by the available x-ray, Raman and thermogravity data [32]. This is a carbon-
365 sulphur composite obtained by reducing graphene oxide (GO) at 600 °C in sulphur vapour.
366 Since the compound appears to be a promising cathode material for Li-S batteries, our C_xS
367 material might as well be suitable for energy storage devices. Using the high pressure
368 technique applied in this study, the material can be easily produced in cm^3 quantity and –

apart from its academic interest - might have interesting other technological application similar to other nanometric 2D graphene-type materials [33,34]. The availability of a material with high surface to weight ratio, with physical properties which can be tailored through its sulphur stoichiometry and which is easily dispersible in an aqueous alcohol solution could find applications for gas sensors, membranes and supercapacitors [33,34].

Data Availability. All data are included in the manuscript and available from the corresponding author upon request and will be deposited on the CNRS cloud https://mycore.core-cloud.net/

References:

[1] R.J. Hemley, Effect of Pressure on Molecules, Annual Rev. of Phys. Chem. 51 (2000) 763-800.

[2] M.J. Lipp, W.J. Evans, B.J. Baer & C-S. Yoo, *Nature Materials* 4 (2005), 211-215.

[3] P.W. Bridgman, Freezing parameters and compressions of twenty-one substances to 50,000 kg/cm^2, Proc. Amer. Acad. Arts Sci. 74 (1942) 399-424

[4] B. Ochiai, & T. Endo, Carbon dioxide and carbon disulphide as resources for functional polymers. Prog. Polym. *Sci.* 30 (2005) 183-215.

[5] E. Whalley, Structure of Bridgman's black carbon disulphide. Can. J. Chem. 38 (1960) 2105-2108.

[6] E.G. Butcher, M. Alsop, J.A. Weston & H.A. Gebbie, Formation and properties of the black form of carbon disulphide. Nature 199 (1963) 756-758.

[7] W.S. Chan & A.K. Jonscher, Structure and electronic properties of solid polymeric carbon disulphide. Phys. stat. sol. 32 (1969) 749-761.

[8] R.P. Dias, Ch.-Sh. Yoo, M. Kim J.S. & Tse, Insulator-metal transition of highly compressed carbon disulphide. Phys. Rev. B 84 (2011), 144104 (6 p.)

[9] F. Bolduan, H.D. Hochheimer, H.J. Jodl, High pressure Raman study of solid CS_2, J. Chem. Phys. 84 (1986) 6997-7004.

[10] S.F. Agnew, R.E. Mischke, B.I. Swanson, Pressure- and Temperature-Induced Chemistry of Carbon Disulfide. J. Phys. Chem. 92 (1988) 4201-4204.

[11] J. Yan, O. Tóth, W. Xu, X-D. Lius, E. Gregoryanz, Ph. Dalladay-Simpson, Z. Qi, S. Xie, F. Gorelli, R. Martoňák, M. Santoro, J. Phy. Chem. Lett. 12 (2021) 7229-7235.

[12] S. Klotz, *Techniques in High Pressure Neutron Scattering*, CRC Press – Taylor & Francis, Boca Raton, FL, 2013.

[13] T. Hattori et al., Design and performance of high-pressure PLANET beamline at pulsed neutron source at J-PARC. Nucl. Instrum. Methods Phys. Res. Sect. A 780 (2015) 55–67.

[14] J. Rodriguez-Carvajal, Recent advances in magnetic structure determination by neutron powder diffraction, Physica B 192 (1993) 55-59.

[15] S. Klotz et al., Techniques for neutron diffraction on solidified gases to 10 GPa and above: Applications to ND_3 phase IV. Appl. Phys. Lett. 67 (1995) 1188-1190.

[16] P. Juhás and T. Davis, C. L. Farrow, S. J. L. Billinge, *PDFgetX3*: a rapid and highly automatable program for processing powder diffraction data into total scattering pair distribution functions. J. Appl. Crystallogr. 46 (2013), 560-566.

411 [17] N.C. Baenziger, W.L. Duax, Crystal Structure and Molecular Motion of Solid Carbon
412 Disulfide, J. Chem. Phys. 48 (1968) 2974-2981.

413 [18] R.J. Nemanich, S.A. Solin, First- and second-order Raman scattering from finite-size
414 crystals of graphite. Phys. Rev. B 20 (1979) 392-401.

415 [19] F. Tuinstra, J.L. Koenig, Raman Spectrum of Graphite. J. Chem. Phys. 53 (1970) 1126-1130.

416 [20] A. Gupta, G. Chen, P. Joshi, S. Tadigadapa, P.C. Eklund, Raman Scattering from High-
417 Frequency Phonons in Supported n-Graphene Layer Films, Nano Lett. 6 (2006) 2667-2673.

418 [21] A.J. Jackson, D. Tiana, A. Walsh, A universal chemical potential for sulfur vapours. Chem.
419 Sci. 7 (2016) 1082-1092.

420 [22] R.J. Nemanich, G. Lucovsky, S.A. Solin, Infrared active vibrations of graphite. Solid State
421 Commun. 23 (1977) 117-120.

422 [23] A. Burian, J.C. Dore, H.E. Fischer, J. Sloan, Structural studies of multiwall carbon nanotubes
423 by neutron diffraction. Phys. Rev. B 59 (1999) 1665-1668.

424 [24] O. Degtyereva, E.R. Herndandez, J. Serrano, M. Somayazulu, H.-k. Mao, E. Gregoryanz,
425 R.J. Hemley, Vibrational dynamics and stability of the high-pressure chain and ring phases in S
426 and Se, J. Chem. Phys. 126 (2007) 084503.

427 [25] N. Sheppard, The vibrational spectra of some organic sulphur compounds and the
428 characteristic frequencies of C-S linkages. Trans. Faraday Soc. 46 (1950) 429-439.

429 [26] Y.N.F. Yuan, R.A. Eaton, A. Anderson, Far infrared study of carbon disulphide at high
430 pressure. Chem. Phys. Lett. 269 (1997) 305-308.

[27] F. Cataldo, A study on the structure and properties of polymeric sulfur, Die Angewandte Makromolekulare Chemie 249 (1997) 137-149.

[28] F. Tuinstra, The structure of insoluble sulfur S_ω, Physica 34 (1967) 113-125.

[29] M. Stolz, R. Winter, W.S. Howells, R.L. McGreevy, P.A. Egelstaff, The structural properties of liquid and quenched sulphur II, J. Phy.: Condens. Matter 6 (1994) 3619-3628.

[30] N.F. Mott, Conduction in non-crystalline materials. Philosophical Magazine, 19 (1969) 835-852.

[31] S.S. Naghavi, Y. Crespo, R. Martoňák, E. Tosatti, High-pressure layered structure of carbon disulphide. Phys. Rev. B 91 (2015) 224108.

[32] S. Zheng, Y. Weng, Y. Zhu, Z. Han, J. Wang, J. Yang, C. Wang, In Situ Sulfur Reduction and Intercalation of Graphite Oxide for Li-S Battery Cathodes. Adv. Energy Mater. 4 (2014) 1400482 (9 p.)

[33] F. Perrozzi, S. Prezioso, L. Ottaviano, Graphene oxide: from fundamentals to applications, J. Phys.: Condens. Matter 27 (2015) 013002 (21 p.).

[34] A.T. Smith, A.M. LaChance, S. Zeng, B. Liu, L. Sun, Synthesis, properties, and applications of graphene oxide/reduced graphene oxide and their nanocomposites, Nano Materials Science 1 (2019) 31–47.

Acknowledgments and Funding Information

S.K. is grateful to J. Biscaras (IMPMC) and D. Hrabovski (Sorbonne Université) for help in the conductivity measurements, S. Renaudineau (Sorbonne Université) for access to the

thermogravimetric equipment, and F. Skouri-Panet (IMPMC) for using the centrifuge. The SEM facility at IMPMC was supported by Région Ile de France Grant SESAME 2006 NOI-07-593/R, Institut National des Sciences de l'Univers (INSU)–CNRS, Institut de Physique–CNRS, Sorbonne Université, and the French National Research Agency (ANR) grant ANR-07-BLAN-0124-01. The neutron scattering experiments were performed at the Japanese neutron spallation source MLF under proposals 2020B0188 and 2021I0011. S.K. wishes to thank Prof. J. A. Gonzalez Gomez (Universidad de Cantabria, Spain) for discussions on Raman data presented here.

CRediT authorship contribution statement

S. Klotz: Writing – original draft, designed the experiment and wrote the paper with contributions from all authors, carried out the Raman and resistivity measurements, produced and prepared all samples. **B. Baptiste**: Formal analysis, carried out the x-ray measurements and the pdf analysis. **T. Hattori**: Formal analysis, carried out the neutron measurements and the pdf analysis. S.M. Feng: Produced three samples during a visit of S.K. at IOP Beijing in 2019. **Ch Jin**: Produced three samples during a visit of S.K. at IOP Beijing in 2019. **K. Béneut**: assisted in the Raman and IR measurements. **J.M. Guigner**: carried out the TEM measurements. **I. Estève**: carried out the SEM measurements.

Graphical abstract